CircRPPH1 accelerates the proliferation and migration of bladder cancer via enhancing the STAT3 signaling pathway

XIAO LIU, YONGHUA TONG, QIU HUANG, YU HE, HAOJIE SHANG, ZHIQIANG CHEN and KUN TANG

Department of Urology, Tongji Hospital, Tongji Medical College, Huazhong University of Science and Technology, Wuhan, Hubei 430030, P.R. China

Received June 1, 2022; Accepted November 7, 2022

DOI: 10.3892/or.2023.8540

Abstract. Bladder cancer (BCa) is a common malignant disease with high recurrence and variable prognosis. Circular RNAs (circRNAs) are implicated in the development of multiple diseases. However, the biological activities of circRNAs in BCa remain largely elusive. In the present study, it was found that circRPPH1 was upregulated in BCa cell lines compared with normal urothelial cells. CircRPPH1 downregulation could inhibit the proliferation, migration and invasion of BCa cells *in vitro* and *in vivo*. Mechanistically, it was demonstrated that circRPPH1 can act as a sponge of miR-296-5P to upregulate STAT3, and interact with FUS to promote phosphorylated (p)-STAT3 nuclear transport. Overall, circRPPH1 could promote BCa progression through sponging miR-296-5p to upregulate the expression of STAT3 and interacting with FUS to promote p-STAT3 nuclear transport. CircRPPH1 was first identified to play a tumorigenic role in BCa, which could be an underlying therapeutic target.

Introduction

Bladder cancer (BCa) is the fourth most common tumour in males, with a high rate of occurrence and recurrence (1). Currently, the development of urinary cytology, cystoscopy, laparoscopic surgery and immune therapy has promoted the diagnosis and treatment of BCa patients. However, problems such as recurrence, metastasis and drug resistance still exist and need to be solved (2). Previous studies have suggested that the progression of BCa closely correlates with the imbalance of genes and signaling pathways (3). Hence, there is a need to explore new therapeutic targets for BCa to obtain improved prognosis.

Circular RNAs (circRNAs) are a kind of non-coding RNAs with tissue-specific expression patterns. Compared with mRNAs, the covalently closed structure of circRNAs contribute to the stability and resistance to degradation (4). The development of sequencing technology has improved our understanding of circRNAs, and a growing number of circRNAs have been identified as important molecules that were involved in in the pathological process of BCa (5). For example, circRNA BCRC-3 was reported to inhibit BCa proliferation through miR-182-5p/p27 axis, while circLIFR could synergize with MSH2 and attenuate chemoresistance in BCa (6,7). Moreover, circRNAs have been proven to possess multiple functions: i) As sponges for miRNA (8); ii) Serving as protein baits or antagonists (9); iii) Adjusting alternative splicing (10); and iv) Translated into polypeptides (11).

The Janus kinase (JAK)/signal transducer and activator of transcription 3 (STAT3) signaling pathway is closely related to the cancer progression. The intrinsic activation of STAT3 has been demonstrated in numerous human solid malignancies (12). After activation by JAKs, p-STAT3 could promote the transcription of target genes after translocating to the nucleus. Additionally, STAT3 is a central intracellular node that integrates signals from EGFR, RAS-RAF-mitogen activated protein kinase, C-MET, and TGF-β pathways, thereby forming a complicate oncogenic signal network (13). In fact, several studies have found that STAT3 is extensively involved in the growth, metastasis and chemotherapy resistance of BCa (14,15).

In the present study, bioinformatics analysis was used to explore the expression of circRNAs in BCa tissues, indicating that circRPPH1 was significantly upregulated in BCa cells. Then, the potential function and mechanism of circRPPH1 in BCa were further investigated through a series of experiments. The results indicated that circRPPH1/STAT3 axis plays a key role in BCa progression. Therefore, CircRPPH1 may be a therapeutic target of BCa.

Correspondence to: Dr Kun Tang or Dr Zhiqiang Chen, Department of Urology, Tongji Hospital, Tongji Medical College, Huazhong University of Science and Technology, 1095 Jiefang Avenue, Wuhan, Hubei 430030, P.R. China
E-mail: tangsk1990@163.com
E-mail: zhqchen_8366@163.com

Abbreviations: BCa, bladder cancer; circRNAs, circular RNAs; JAK, Janus kinase; STAT3, signal transducer and activator of transcription 3; p-STAT3, phosphorylated STAT3; RT-qPCR, reverse transcription-quantitative polymerase chain reaction; cDNA, complementary DNA; WT, wild-type; MUT, mutant-type; FISH, fluorescence *in situ* hybridization; PBS, phosphate-buffered saline; CCK-8 assay, Cell Counting Kit-8 assay; RIP assay, RNA immunoprecipitation assay; co-IP assay, co-immunoprecipitation assay; H&E, Haematoxylin and eosin; IHC, immunohistochemistry

Key words: circular RNA, circRPPH1, bladder cancer, function, STAT3

Materials and methods

Cell culture. Human BCa cell lines (T24 and 5637) were purchased from Procell Life Science & Technology Co., Ltd. The human normal urothelial cell line SV-HUC-1 and 293T cell line were obtained from the Cell Bank of the Chinese Academy of Science (Shanghai, China) and maintained in our laboratory. Both BCa cells were cultured in RPMI-1640 medium (Gibco; Thermo Fisher Scientific, Inc.). SV-HUC-1 cells were maintained in the F-12 K medium (Gibco; Thermo Fisher Scientific, Inc.), while 293T cells were cultured in DMEM (Gibco; Thermo Fisher Scientific, Inc.). The aforementioned cell mediums were supplemented with 10% fetal bovine serum (Gibco; Thermo Fisher Scientific, Inc.). All cells were incubated in a humidified incubator at 37˚C with 5% CO_2.

Bioinformatics analysis. The differentially expressed circRNA data (GSE92675 and GSE97239) in BCa were downloaded from the GEO database (https://www.ncbi.nlm.nih.gov/geo/) (16,17), while hierarchical clustering analysis was performed by Cluster3.0 software (http://bonsai.hgc.jp/~mdehoon/software/cluster/software.htm) and visualized with Java TreeView software (http://jtreeview.sourceforge.net). To predict the potential circRNA-miRNA and mRNA-miRNA interactions, circBank (18), circinteractome (19), and TargetScan (20) were used according to the corresponding instructions. Furthermore, RNAfold Web Server (http://rna.tbi.univie.ac.at/cgi-bin/RNAWebSuite/RNAfold.cgi), RNACOmposer (http://rnacomposer.ibch.poznan.pl/), Protein Data Bank (https://www.rcsb.org/), and HDOCK (http://hdock.phys.hust.edu.cn/) were used to predict the binding between circRPPH1 and FUS protein.

Vector construction. The PCDH-H1 shRNA cloning vector was used to construct circRPPH1 knockdown (shRNA#1, shRNA#2, shRNA#3) plasmids and FUS knockdown plasmid. The construction of the PCDH-H1 plasmid was previously described by the authors (21). Gene-specific shRNA target sequences were synthesized by Tsingke Biological Technology. These shRNA sequences all contain the sequences of restriction enzymes. Then, these shRNA sequences were annealed and cloned into the PCDH-H1 plasmid. In the construction of overexpression plasmids, the circRPPH1 sequence was cloned into the pLC5-circ vector (Guangzhou Geneseed Biotech Co., Ltd.). Moreover, a second-generation lentiviral system was applied for the production of lentiviruses. A total of 24 μg plasmids were used for lentivirus packaging, and the ratio of lentivirus plasmid: target plasmid: pHelper 1.0: pHelper 2.0 was 2:1:1. After ~48 h of transfection, the lentiviruses were collected and used to infect BCa cells (MOI=5). After 72 h, BCa cells were further cultured with fresh culture medium containing puromycin (2 μg/ml) for 5 days to establish the stable interference or overexpression systems in BCa cells. Both pHelper 1.0 plasmid and pHelper 2.0 plasmid were obtained from GeneChem (Shanghai, China).

The luciferase reporter assays were performed with the psiCHECK2 vector (Shanghai GenePharma Co., Ltd.). All of the wild-type (WT) and mutant (MUT) sequences were directly synthesized by Tsingke Biotechnology (Beijing, China). Then, each sequence was cloned into the polyclonal site region of the vector. Besides, miR-296-5p mimic or inhibitor and their negative controls were provided by Tsingke Biological Technology. The final working concentration of miRNA inhibitor, miRNA mimic, or negative controls was 50 nM. When the cell density reached 70%, the oligonucleotides were transfected using Lipofectamine® 3000 (Thermo Fisher Scientific, Inc.) according to the manufacturer's protocol. Following 48 h of transfection at 37˚C, the cells were used for further detection. All oligonucleosides used in the present study are provided in Table SI. All plasmids were verified by sequencing.

Reverse transcription-quantitative (RT-q) PCR. Total RNA was isolated with TRIzol Reagent (Sangon Biotech Co., Ltd.), following the manufacturing protocol. For circRNA and mRNA, the complementary DNA (cDNA) was generated using the HiScript® III 1st Strand cDNA Synthesis kit (Vazyme Biotech Co., Ltd.) according to the manufacturing protocol and the miRNA First Strand cDNA Synthesis kit (Sangon Biotech Co., Ltd.) was used to synthesize cDNA for miRNA. Next, quantification of RNA was performed with a SYBR Green PCR kit (Shanghai Yeasen Biotechnology Co., Ltd.) according to the manufacturing protocol. The conditions for PCR amplification were as follows: 5 min at 95˚C for one cycle, followed by denaturation for 10 sec at 95˚C and extension for 30 sec at 60˚C for 40 cycles. The $2^{-\Delta\Delta Cq}$ method was used to determine the fold change of expression (22). All primers were designed by ourselves and synthesized by Tsingke Biological Technology. Notably, the design of the circRPPH1-divergent forward primer required coverage of the back-splice point of circRPPH1. The sequences of all primers were provided in Table SII. The circRPPH1, STAT3 or miR-296-5p expression was normalized to GAPDH or U6, respectively. Additionally, cytoplasmic and nuclear RNA was extracted by Thermo Fisher BioReagents (Thermo Fisher Scientific, Inc.).

RNase R treatment and Actinomycin D assay. To evaluate the stability of circRPPH1, RNase R (Beyotime Institute of Biotechnology) and actinomycin D (MedChemExpress) were used. Firstly, the 15 U RNase R was used to treat total RNA (5 μg) at 37˚C for 1 h. Then, the levels of circRPPH1 and linear RPPH1 RNA was detected by RT-qPCR. Additionally, cells were exposed to actinomycin D (10 μg/ml) for different time intervals (0, 3, 6, 9 and 12 h). The circRPPH1 expression levels were also determined with RT-qPCR. Notably, PCR products of circRPPH1 were applied to Sanger sequencing.

Fluorescence in situ hybridization (FISH). Using a FISH kit (cat. no. F12201/50; Shanghai GenePharma Co., Ltd.), FISH assays were performed following the manufacturer's protocol. In brief, tumor cells were seeded in confocal petri dishes and cultured to 80% confluence. The dishes were then washed twice with phosphate-buffered saline (PBS), fixed with 200 μl 4% paraformaldehyde at room temperature for 15 min, and permeabilized with 200 μl 0.1% Triton X for 15 min at room temperature. After washing twice with PBS, 200 μl of 2X sodium citrate buffer (SSC) solution was added to each dish at 37˚C for 30 min. Then, the dishes were incubated in 200-μl denatured probe mixture in a humidified incubator at 37˚C overnight. The next day, the dishes were washed with a solution of 0.1% Tween-20 in 4X SSC for 5 min, a solution of

0.1% Tween-20 in 2X SSC for 5 min, and a solution of 0.1% Tween-20 in 1X SSC for 5 min at 42˚C in dark. After that, DAPI working solution (1:10,000) was added into the dishes for 15 min in dark. Finally, the dishes were washed twice with PBS. The pictures were captured directly using an immunofluorescence microscope. All probes were provided by Shanghai GenePharma Co., Ltd.

Cell Counting Kit-8 (CCK-8) and colony formation assay. The proliferation ability of BCa cells was assessed with different experiments. Firstly, the CCK-8 assay was conducted with T24 or 5637 cells seeded in a 96-well plate at a density of $2x10^3$ cells per well. After cell attachment to the wall, 10 μl CCK-8 solution (Beyotime Institute of Biotechnology) was added at different time points (0, 24, 48 and 72 h) and incubated at 37˚C for 1 h. Finally, absorbance was measured at 450 nm.

During the colony formation assay, $2x10^3$ cells were seeded in six-well plates and incubated at 37˚C for 14 days. The medium was replaced every 5 days. Then, the colonies (>50 cells) were sequentially fixed with 100% methanol at room temperature for 30 min and stained with 0.1% crystal violet at room temperature for 15 min. The cells were manually counted under a dissecting microscope and the colony formation efficiency was calculated (number of colonies/number of cells inoculated x100%).

Cell invasion and migration assay. Cell invasion or migration abilities were measured using 8-μm pore size Transwell chambers (Corning, Inc.). For invasion assays, upper chambers were pre-coated with Matrigel (1:8; BD Biosciences) for 1 h at room temperature. The upper chamber was inoculated with a cell suspension ($3x10^5$ cells/ml) and cultured with serum-free medium, while the lower chamber was supplemented with medium containing 10% FBS. The cells were incubated at 37°C for 12 h. After 12 h of incubation, cells in the lower chamber were fixed with 4% paraformaldehyde at room temperature for 30 min and stained with 0.1% crystal violet at room temperature for 15 min. Then, pictures were captured by a light microscope (Olympus Corporation). The number of invasive cells were counted in 5 randomly selected visual fields in each group.

Luciferase reporter assay. The WT or MUT luciferase reporter plasmids were co-transfected into 293T cells along with miR-NC and miR-296-5p mimic. Following transfection for 36 h, the cells were harvested and lysed, then the supernatant was collected. Dual Luciferase Reporter Gene Assay kit (Shanghai Yeasen Biotechnology Co., Ltd.) was used to measure the dual Luciferase activity of each sample with ~20 μl supernatant. The internal control was firefly luciferase reporters co-expressed on psiCHECK2 plasmids.

RNA immunoprecipitation (RIP) assay. An RNA Immunoprecipitation kit (cat. no. P0102; Guangzhou Geneseed Biotech Co., Ltd.) was used to perform the RIP assays. In accordance with the manufacturer's protocol, 100 μl protein A/G beads were first conjugated to antibodies against FUS (1:50), AGO2 (1:50) or IgG (1:50). After that, the cell extracts were mixed with A/G protein beads. Finally, qPCR was used to analyze the precipitated RNAs.

Western blotting, co-immunoprecipitation (co-IP) and antibodies. The total protein was extracted using RIPA lysis buffer (Sangon Biotech Co., Ltd.), while the nuclear protein was extracted using a Nuclear Protein Extraction kit (Beijing Solarbio Science & Technology Co., Ltd.). Protein concentrations were measured using a BCA protein assay kit (Wuhan Servicebio Technology Co., Ltd.). Total proteins (20 μg) were separated by 10% sodium dodecyl-sulfate polyacrylamide gel electrophoresis. Then, the proteins were transferred to nitrocellulose membranes and blocked with 5% skim milk (Yili; https://oceaniadairy.co.nz/yili-group/) or 5% BSA (Wuhan Servicebio Technology Co., Ltd.) at room temperature for 60 min. After that, the membrane was incubated with primary antibodies against STAT3 (1:1,000), phosphorylated STAT3 (1:1,000), FUS (1:1,000), Histone H3 (1:2,000), or GAPDH (1:2,000, cat. no. AC001; Abclonal Biotech Co., Ltd.) at 4˚C overnight. Next, membranes were incubated with HRP-conjugated goat anti-rabbit (1:10,000; cat. no. ab288151; Abcam) or goat anti-mouse secondary antibodies (1:10,000; cat. no. ab97040; Abcam) at room temperature for 60 min. Finally, the immunoreactive blot was visualized with enhanced chemiluminescence reagent (Wuhan Servicebio Technology Co., Ltd.).

Co-immunoprecipitation (co-IP) was conducted with a magnetic IP kit (cat. no. 88804; Thermo Fisher Scientific, Inc.). Briefly, cell lysates were gently rotated overnight with anti-FUS antibody, anti-STAT3 antibody or normal rabbit IgG (Beyotime Institute of Biotechnology). Afterwards, pre-washed protein A/G magnetic beads were incubated with rotating for 1 more h. The beads were collected and washed three times. Western blotting was performed after eluting bound proteins with elution buffer. All antibodies used in the present study are listed in Table SIII.

Haematoxylin and eosin (H&E) and immunohistochemical (IHC) staining. Tissues embedded in paraffin were sectioned to a thickness of 5 μm, deparaffinized using xylene and rehydrated using a graded series of ethanol. H&E was applied to one section according to standard procedures. Other sections were stained for IHC. IHC was performed by incubating sections with primary antibodies at room temperature for 2 h. Anti-STAT3 rabbit polyclonal antibody and anti-Ki67 rabbit polyclonal antibody were used as primary antibodies at concentrations of 10 and 5 μg/ml, respectively. The next step involved adding HRP-conjugated goat anti-rabbit (1:500; cat. no. ab288151; Abcam) for 30 min at 37˚C, followed by streptavidin labelled with peroxidase. Antibody staining was revealed using chromogen 3,3-diaminobenzidine. Moreover, non-specific immunoglobulin was used as the negative control. Finally, the slides were observed under a light microscope (Olympus Corporation).

In vivo study. This animal experiment was approved (approval no. TJH-202110004) by the Animal Research Ethics Committee of Tongji Hospital (Wuhan, China). The experimental procedure and animal care were all in line with the National Institutes of Health Guide for the Care and Use of Laboratory Animals. Female nude mice (n=10, 4 weeks old, weight 19-25 g) were purchased from Beijing Vital River Laboratory Animal Technology Co., Ltd. and housed in a

pathogen-free facility (26˚C; 50% humidity; 12-h light/dark cycle with food and water provided *ad libitum*). The experimental animals were randomly divided into sh-circrRPPH1 group and sh-NC group (5 mice per group). Cells ($1x10^7$) were suspended in 200 μl PBS and injected into the right back region of nude mice. Mice were under daily monitoring. The tumor size was measured with calipers at 7, 14, 21 and 28 days after inoculation. The largest tumor diameter allowed in this experiment was <20 mm. After 30 days, the nude mice were euthanized by pentobarbital sodium (100 mg/kg) via intravenous injection and verified the sacrifice by cessation of breathing and heartbeat. Then, the weight of the excised tumor was recorded. Moreover, HE and IHC staining were applied to study tumor tissues.

To establish the lung metastasis model, 4 weeks old BABL/C female nude mice were randomly divided into sh-circRPPH1 group and sh-NC group (5 mice per group). Single cells ($2x10^6$) were suspended in 100 μl PBS and injected into the tail vein of nude mice. After 6 weeks, mice were euthanized with sodium pentobarbital (100 mg/kg), and lung tissue was obtained. The resected lungs were subjected to H&E and IHC staining. Then, the metastatic lesions in lung were carefully examined by 3 pathologists.

Statistical analysis. Statistical analysis in the present study was performed using the SPSS 26.0 package program (IBM Corp.). The statistical significance between the two groups was calculated using the unpaired Student's t-test, while the statistical significance between the three or more groups was calculated using one-way ANOVA followed by Tukey's multiple comparison test. Data were expressed as the mean ± standard deviation (SD) of three independent experiments. Moreover, differences were considered statistically significant when $P<0.05$.

Results

The expression profiles and characteristics of circRPPH1. An increasing number of public databases are constructed to facilitate cancer research. To identify critical circRNAs involved in BCa tumorigenesis, the expression patterns of circRNAs were analyzed with two GEO datasets (GSE97239 and GSE92675) and a variety of circRNAs aberrantly expressed in BCa were found (Fig. 1A and B). A total of 4 overlapping differentially expressed circRNAs exist between these two databases, including hsa_circ_0000824, hsa_circ_0004368, hsa_circ_0006117, and hsa_circ_0000512 (Fig. 1C). Among them, circRPPH1 (hsa_circ_0000512) was the only one upregulated circRNA and was selected for further exploration (Fig. 1D).

Next, the expression levels of circRPPH1 were compared between BCa cells and normal human bladder epithelial cells. Compared with normal human bladder epithelial cells, circRPPH1 was significantly higher in BCa cells (Fig. 2A). In addition, circRPPH1 is generated from exon of the RPPH1 gene located on chr14: 20,811,283-20,811,436. The special sequences in the back-spliced junction point of circRPPH1 were verified by Sanger sequencing (Fig. 2B). Next, the circular structure of circRPPH1 was confirmed by RT-qPCR and agarose gel electrophoresis using convergent and divergent primers. As expected, divergent primers could amplify circRPPH1 in cDNA rather than genomic DNA (Fig. 2C). Compared with parental linear genes, circRNAs are more resistant to the degradation of RNase R because of their unique circular structure (4). In fact, circRPPH1 also exhibited resistance to RNase R in the present study, while the linear RPPH1 RNA or GAPDH mRNA were significantly degraded after RNase R treatment (Fig. 2D). Similarly, the results of RT-qPCR after actinomycin D treatment showed that the degradation rate of circRPPH1 was lower than that of the linear transcript (Fig. 2E). Moreover, the nuclear-cytoplasmic separation assay and FISH experiments indicated that most of the circRPPH1 was located in the cytoplasm (Fig. 2F and G). In brief, these results indicated that circRPPH1 is upregulated in BCa cells and is primarily located in the cytoplasm.

CircRPPH1 promotes the proliferation and invasion of BCa cells in vitro. To evaluate the biological functions of circRPPH1 in BCa cells, three interference plasmids (sh-circRPPH1#1, sh-circRPPH1#2 and sh-circRPPH1#3) and one overexpression plasmid were constructed. It was found that transient transfection of sh-circRPPH1 #2 or OE-circRPPH1 could significantly change the expression level of circRPPH1, while sh-circRPPH1#1 and sh-circRPPH1#3 had relatively weak effects. Then, the stable interference or overexpression systems of circRPPH1 was successfully established in T24 and 5637 cells using lentiviral packaging plasmid. Notably, the RNA level of linear RPPH1 was stable while circRPPH1 expression was altered. The aforementioned results are shown in Fig. S1A-E.

The cell viability of BCa cells was detected by CCK-8 assay. The results indicated that circRPPH1 knockdown significantly inhibited the cell viability of T24 and 5637 cells. The clone formation experiments showed that interference of circRPPH1 could significantly inhibit BCa cell proliferation. Conversely, overexpression of circRPPH1 increased the proliferation ability of BCa cells (Fig. 3A and B). Transwell and Matrigel experiments indicated that the migration and invasion abilities of BCa cells were significantly inhibited following circRPPH1 knockdown, while the migration and invasion abilities of BCa cells were enhanced by circRPPH1 overexpression (Fig. 3C and D).

CircRPPH1 sponges miR-296-5p in BCa cells. Considering most circRNAs usually act as miRNA sponges to exert their functions (23), CircInteractome (https://circinteractome.nia.nih.gov/) and CIRCBANK (http://www.circbank.cn/) were searched to predict the miRNAs that can interact with circRPPH1. MiR-615-5p and miR-296-5p were predicted to be the potential target miRNAs (Fig. 4A), and were selected for subsequent experiments. Notably, miR-296-5p but not miR-615-5p levels were affected when circRPPH1 was overexpressed or interfered (Fig. 4B and C). Additionally, the targeted relationship between circRPPH1 and miR-296-5p was further verified by luciferase reporter assays. Compared with the negative control, miR-296-5p mimic reduced the luciferase activity of WT-circRPPH1 plasmid in 293T cells, while the luciferase activity of MUT-circRPPH1 plasmid had little change (Fig. 4D). With RIP assays, circRPPH1 and miR-296-5p were significantly enriched by AGO2 antibodies

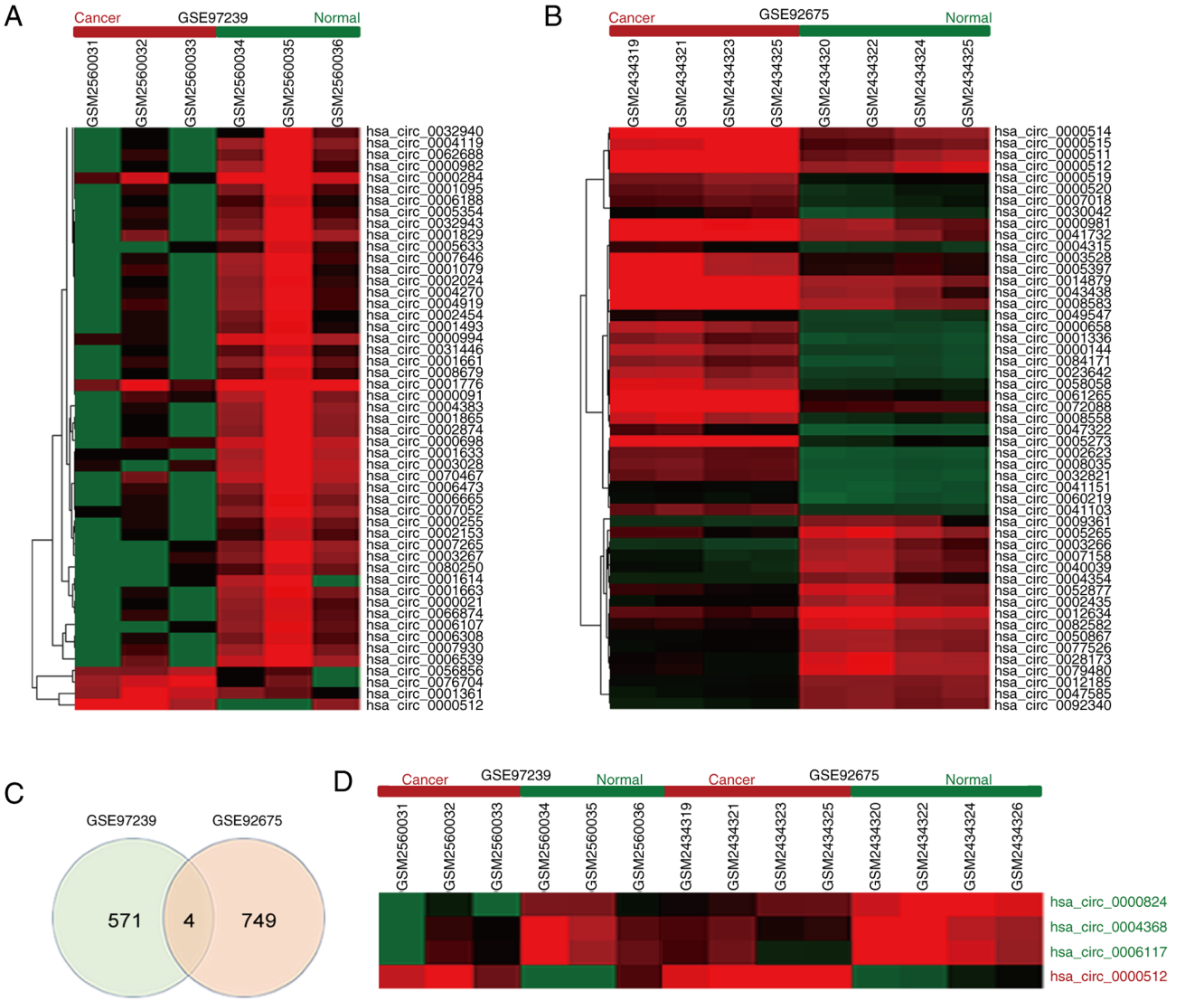

Figure 1. CircRNA profiles in BCa. (A) Heat map and hierarchical clustering analysis of circRNAs differentially expressed between 3 paired BCa and normal bladder tissues in the GSE97239 dataset. (B) Heat map and hierarchical clustering analysis of circRNAs differentially expressed between 4 paired BCa and normal bladder tissues in the GSE92675 dataset. (C) Venn analysis showing the four overlapping differentially expressed circRNAs between the two datasets. (D) Heat map and hierarchical clustering analysis of the overlapping differentially expressed circRNAs between the two datasets. CircRPPH1 (hsa_circ_0000512) was the only one upregulated circRNA. BCa, bladder cancer; circRNA, circular RNA; hsa, *Homo sapiens*.

(Fig. 4E) Collectively, circRPPH1 probably functioned as a sponge of miR-296-5p.

MiR-296-5p targets STAT3 and suppresses the proliferation and invasion of BCa cells. Based on the TargetScan (http://www.targetscan.org), miR-296-5p was predicted to bind to the 3' untranslated region of STAT3 mRNA with a high-score. The luciferase reporter assays were applied to testify this interaction. Compared with miR-NC, miR-296-5p mimic could significantly reduce the luciferase activity of WT-STAT3, whereas the luciferase activity of MUT-STAT3 was not affected by miR-296-5p mimic (Fig. 5A). Furthermore, it was found that miR-296-5p overexpression could significantly reduce the expression of STAT3 by RT-qPCR and western blot analysis (Fig. 5B and C).

The effect of miR-296-5p on the malignant biological behaviors was explored. The results showed that overexpression of miR-296-5p inhibited the proliferation (Fig. 5D and E), invasion and migration (Fig. 5F and G) of BCa cells. Additionally, miR-296-5p knockdown exerted an opposite effect (Fig. S2A and B). The transfection efficiencies of miR-296-5p mimic and inh-296-5p were verified with RT-qPCR (Fig. S1H and I). Notably, the transfection efficacy of inh-296-5p was verified by a known target gene (NRG1) from a previous study (24). In conclusion, miR-296-5p could suppress the development of BCa by targeting STAT3.

CircRPPH1 promotes the proliferation and invasion of BCa by sponging miR-296-5p to regulate STAT3. The interaction among circRPPH1, miR-296-5p and STAT3 was further explored. In the luciferase reporter assays, circRPPH1 overexpression significantly increased the luciferase activity of WT-STAT3 plasmid, whereas the miR-296-5p could eliminate this effect. Furthermore, this phenomenon disappeared with MUT-STAT3 plasmid (Fig. 6A). Using western blot analysis and RT-qPCR, the STAT3 mRNA and protein

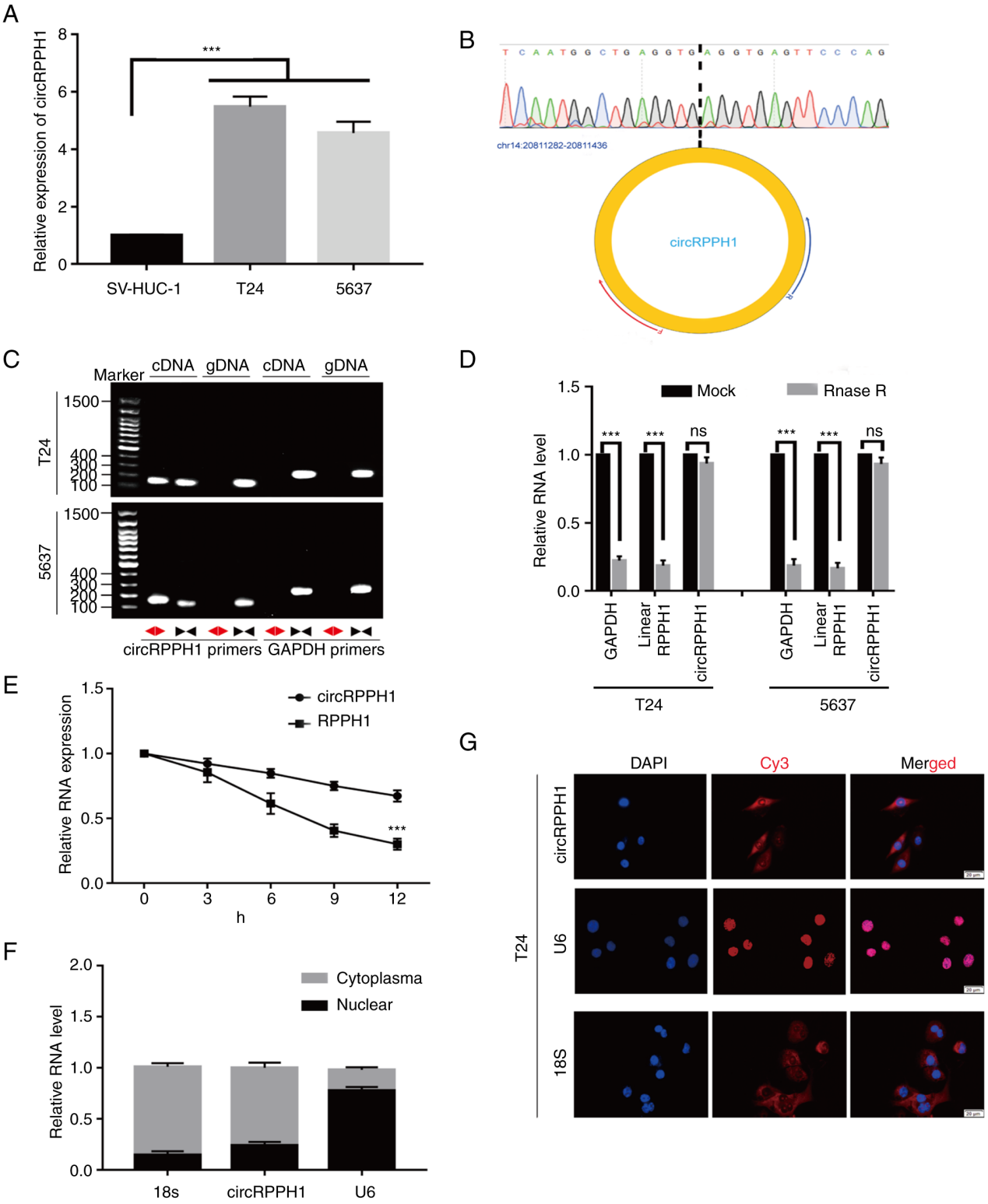

Figure 2. Characteristics of circRPPH1. (A) RT-qPCR was used to detect the circRPPH1 expression in SV-HUC-1, T24 and 5637 cells. (B) The back-spliced junction point of circRPPH1 was validated by sanger sequencing. (C) RT-qPCR using divergent primers could amplify circRPPH1 in cDNA but not genomic DNA, which further verified the existence of circRPPH1. (D) After treatment with or without RNase R, the relative RNA levels were analyzed with RT-qPCR. (E) Compared with the linear RPPH1 RNA level, the circRPPH1 level in BCa cells was significantly higher after treatment with actinomycin D. (F) Identification of circRPPH1 cytoplasmic and nuclear distribution by RT-qPCR analysis in T24 cells. (G) Subcellular localization analysis by fluorescence *in situ* hybridization indicated that circRPPH1 is mainly located in the cytoplasm of BCa cells (scale bar, 20 μm). Data are presented as the mean ± SD. ***P<0.001. circ-, circular; RT-qPCR, reverse transcription-quantitative PCR; BCa, bladder cancer.

levels were significantly increased by circRPPH1 overexpression, while miR-296-5p mimic could cancel out this effect (Fig. 6B and C). The aforementioned results demonstrated that STAT3 expression was regulated by circRPPH1, which is a competing endogenous RNA and sponges miR-296-5p. Several rescue experiments were implemented to further

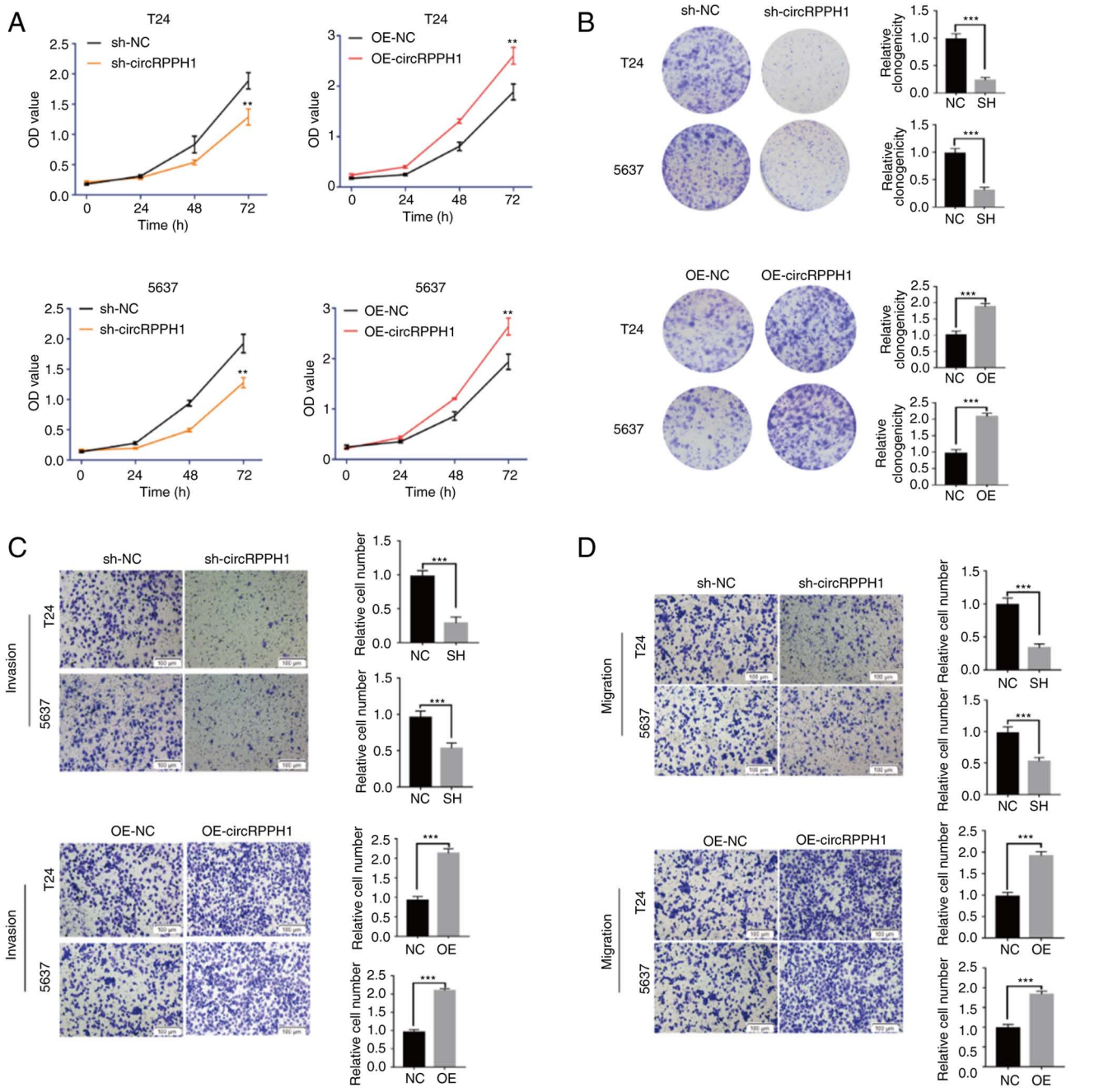

Figure 3. CircRPPH1 promotes the proliferation and invasion of BCa cells. (A and B) The proliferation abilities of BCa cells were evaluated by Cell Counting Kit-8 assay and colony formation assay. (C and D) The Transwell assay was performed for invasion and migration of BCa cells (scale bar, 100 μm). Data are presented as the mean ± SD. **P<0.01 and ***P<0.001. circ-, circular; BCa, bladder cancer; sh-, short hairpin; OE, overexpression; NC, negative control.

verify this complex relationship. The results indicated that circRPPH1 knockdown significantly inhibited the proliferation, invasion and migration abilities of BCa cells. However, co-transfection of sh-circRPPH1 and inh-296-5p may cancel out this effect (Fig. 6D-G). In summary, circRPPH1 accelerates the biological behaviors of BCa cells by sponging miR-296-5p to regulate STAT3 expression.

The interaction of circRPPH1 and FUS facilitates the nuclear translocation of phosphorylated STAT3 in BCa cells. Recently, two studies reported that the binding of FUS to STAT3 promotes the translocation of p-STAT3 into the nuclei (25,26). Moreover, three online databases suggested a potential interaction between circRPPH1 and FUS (Fig. 7A). Then, the interaction between circRPPH1 and FUS was further analyzed on HDOCK (http://hdock.phys.hust.edu.cn/). Firstly, the RNAfold Web Server and RNACOmposer were used to predict the tertiary structure of circRPPH1. Next, the tertiary structure of FUS was acquired from Protein Data Bank (27). Finally, this structure information was imported into the HDOCK. As demonstrated in Fig. 7B, the predicted result further indicated the interaction between circRPPH1 and FUS.

To further explore the interaction among circRPPH1, FUS, STAT3 and p-STAT3, several experiments were conducted. RIP assays were used to verify the interaction of circRPPH1 with FUS protein (Fig. 7C). A co-IP assay verified

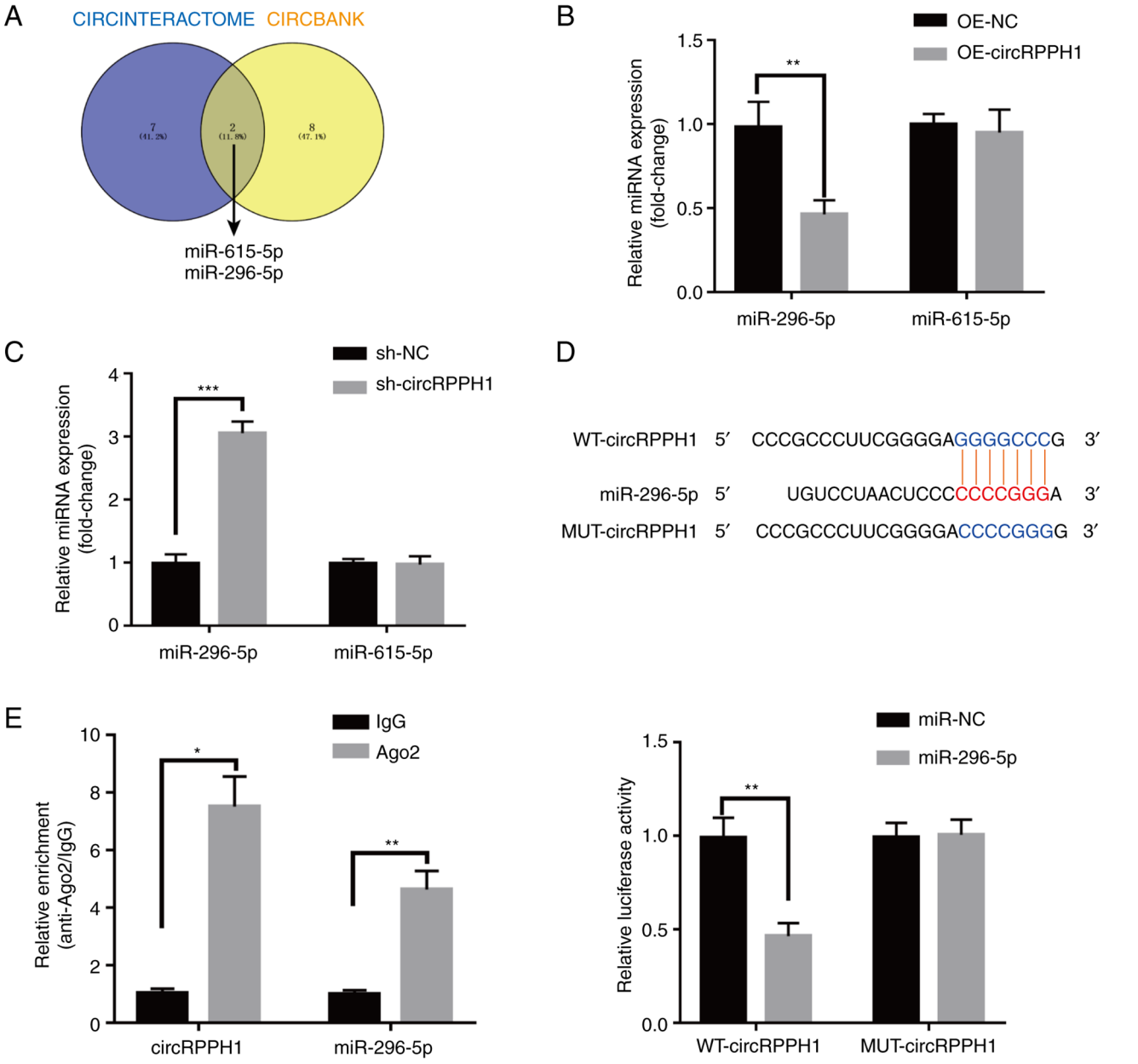

Figure 4. CircRPPH1 directly targets to miR-296-5p and suppresses miR-296-5p activity. (A) miR-296-5p and miR-615-5p were predicted to be the potential targets of circRPPH1 in the Circinteractome and Circbank databases. (B and C) Bladder cancer cells were transfected with OE-NC, OE-circRPPH1, sh-circRPPH1, and sh-NC. After transfection, the expression levels of miR-296-5p and miR-615-5p were analyzed by reverse transcription-quantitative PCR. (D) After co-transfection of luciferase reporter vectors and miR-296-5p mimics or miR-NC into 293T cells, the luciferase activities were detected and analyzed. MiR-296-5p overexpression could significantly inhibit the luciferase activities of WT vector but not MUT vector. (E) CircRPPH1 and miR-296-5p were significantly enriched by AGO2 antibodies in RNA immunoprecipitation assays. Data are presented as the mean ± SD. *P<0.05, **P<0.01 and ***P<0.001. circ-, circular; miR, microRNA; OE, overexpression; sh-, short hairpin; NC, negative control; WT, wild-type; MUT, mutant.

the interaction between FUS and STAT3 (Fig. 7D). Western blotting indicated that FUS knockdown has no effect on the expression of total STAT3 (Fig. 7E). Similarly, FUS knockdown has no effect on the circRPPH1 expression (Fig. S1F and G). It was observed that circRPPH1 overexpression upregulated the STAT3 level and promoted the nuclear translocation of p-STAT3, while FUS knockdown could counteract this effect (Fig. 7F). Next, CCK-8 and Transwell assays further confirmed that the interaction between the FUS and circRPPH1 could promote the proliferation and invasion abilities of BCa cells (Fig. S2C and D). In conclusion, it was demonstrated that the interaction between circRPPH1 and FUS could promote the nuclear translocation of p-STAT3, which further explained the carcinogenic role of circRPPH1.

CircRPPH1 accelerates tumor growth and metastasis in vivo. To further evaluate the effects of circRPPH1 on growth or metastasis *in vivo*, stably transfected BCa cells were injected into the dorsal and tail vein of nude mice, respectively. Tumor volume and weight in the sh-circRPPH1 group were significantly smaller than those in the sh-NC group (Fig. 8A-C). H&E staining was used to further examine these subcutaneous tumors and lung metastases (Fig. 8D and E). Compared with the sh-NC group, the sh-circRPPH1 group had fewer

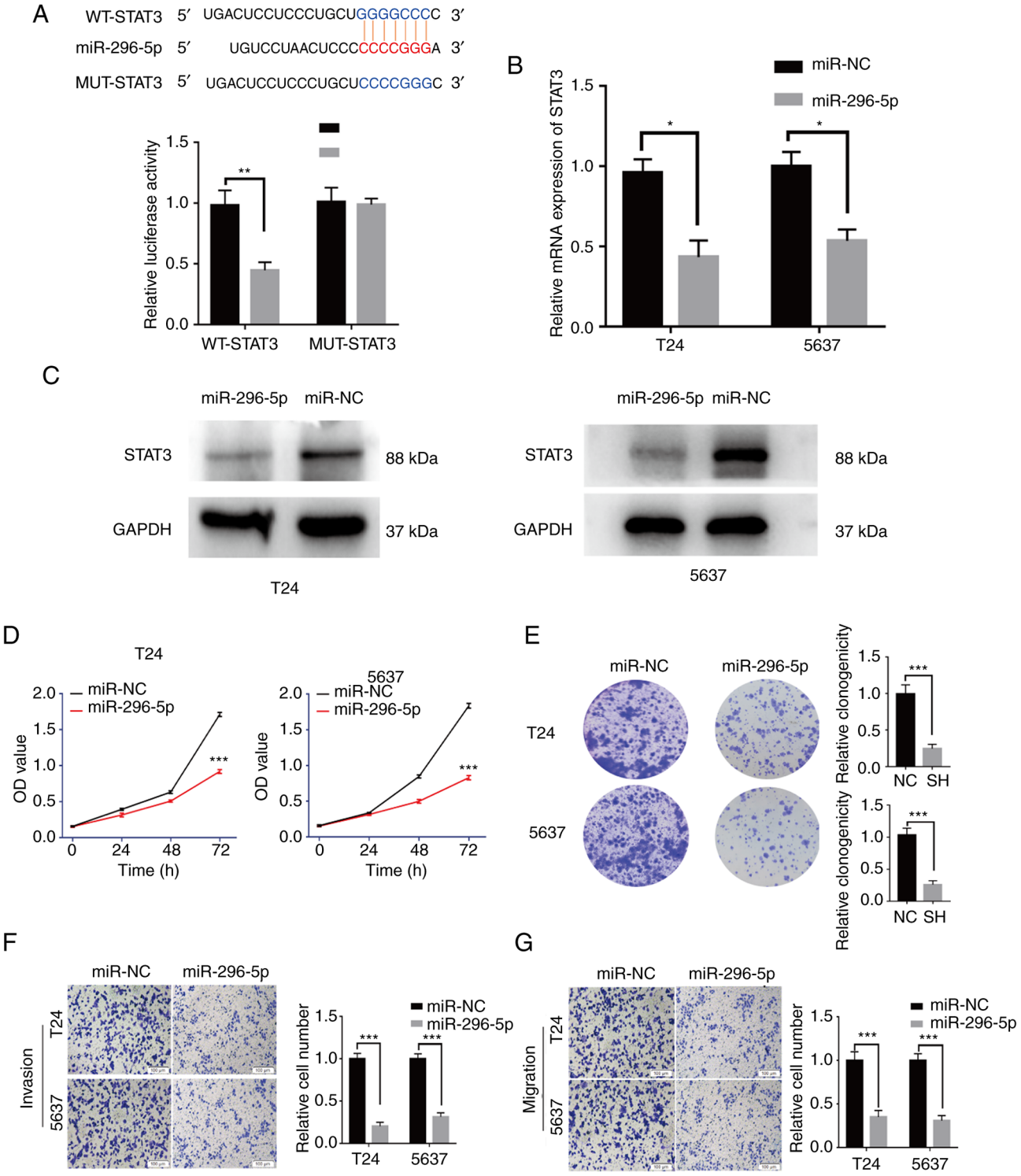

Figure 5. miR-296-5p suppresses BCa cell activities through STAT3. (A) miR-296-5p significantly inhibited luciferase activity in the WT-STAT3 vector, but not in the MUT-STAT3 vector. (B and C) The STAT3 expression was significantly inhibited by miR-296-5p in BCa cells. (D and E) The proliferation abilities of BCa cells transfected with miR-296-5p mimics or miR-NC were assessed by Cell Counting Kit-8 assay and colony formation assay. (F and G) Invasion or migration abilities of BCa cells transfected with miR-296-5p mimics or miR-NC were examined through Transwell and Matrigel assays (scale bar, 100 μm). Data are presented as the mean ± SD. *P<0.05, **P<0.01 and ***P<0.001. miR, microRNA; BCa, bladder cancer; WT, wild-type; MUT, mutant; OE, overexpression; sh-, short hairpin; NC, negative control.

lung metastases. In addition, the results of IHC indicated that STAT3 expressions were significantly downregulated in the sh-circRPPH1 group compared with the sh-NC group (Fig. 8F and G). Collectively, these results indicated that circRPPH1 still acted as an oncogene in xenograft models.

Discussion

BCa is the most common malignant disease in the urinary system with high incidence and recurrence (28). There is growing evidence that circRNAs play important regulatory

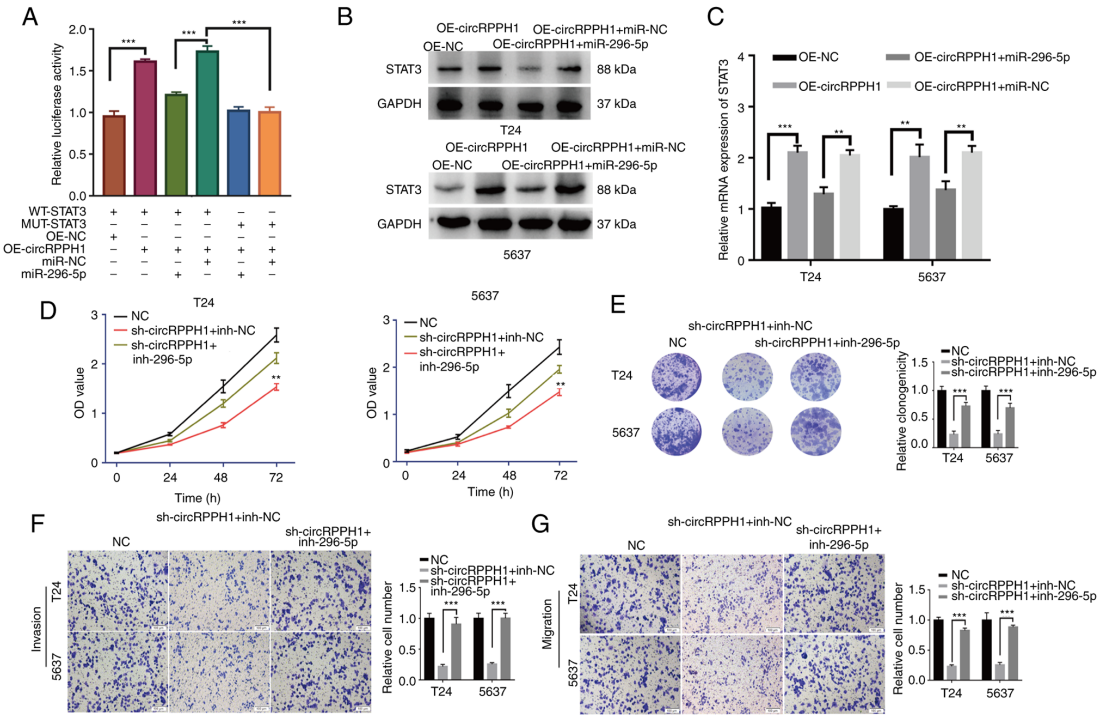

Figure 6. CircRPPH1 promotes the proliferation and invasion of BCa by sponging miR-296-5p to regulate STAT3. (A) The luciferase assays were conducted to explore the interaction among circRPPH1, miR-296-5p and STAT3. CirRPPH1 overexpression significantly promoted the luciferase activities in the WT-STAT3 vectors, while the miR-296-5p mimic could counteract this effect. (B and C) Single transfection of OE-circRPPH1 vectors could significantly upregulate the STAT3 expression levels in BCa cells, while the co-transfection of OE-circRPPH1 and miR-296-5p mimic would cancel out this effect. (D and E) With Cell Counting Kit-8 and colony formation assays, the proliferation abilities of cells were evaluated after co-transfection with circRPPH1 and miR-296-5p mimics. (F and G) Cell invasion and migration abilities was examined in cells co-transfected with circRPPH1 and miR-296-5p mimics (scale bar, 100 μm). Data are presented as the mean ± SD. **P<0.01 and ***P<0.001. circ-, circular; BCa, bladder cancer; miR, microRNA; OE, overexpression; sh-, short hairpin; NC, negative control; inh-, inhibitor.

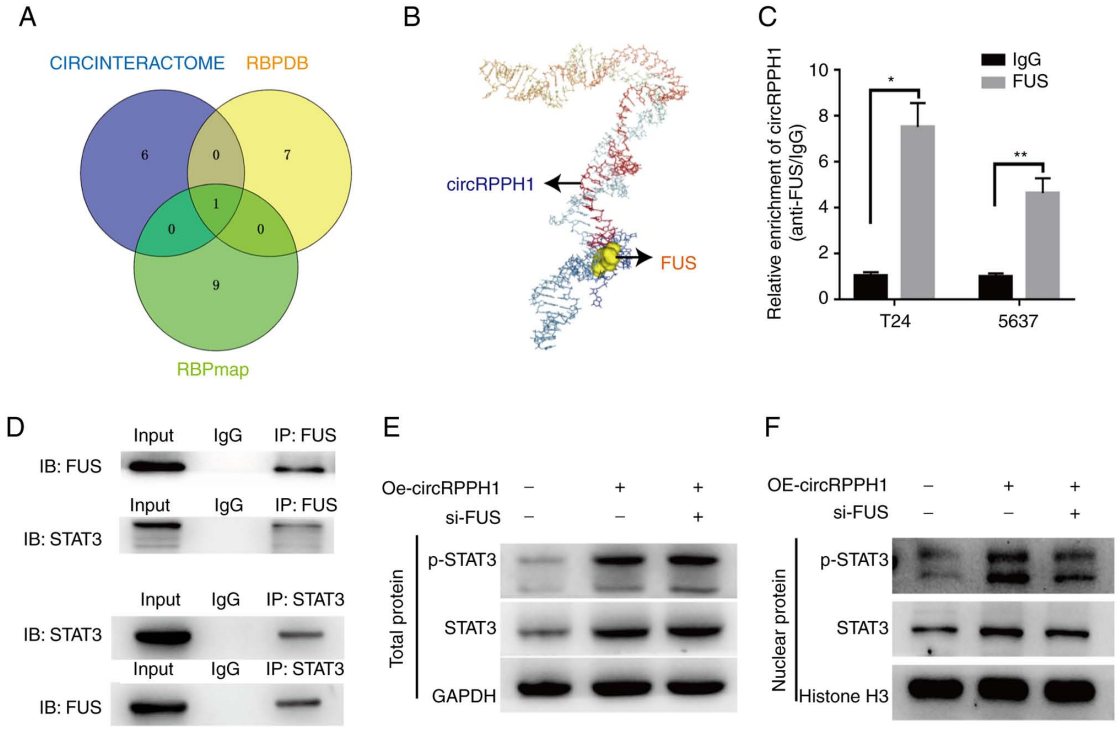

Figure 7. Interaction between circRPPH1 and FUS accelerates the nuclear translocation of p-STAT3. (A) CircRPPH1 was predicted to bind to the FUS protein in Circinteractome, RBPDB and RBPmap databases. (B) Diagrams showing the interaction of circRPPH1 and FUS. (C) CircRPPH1 was significantly enriched by FUS antibodies in the RNA immunoprecipitation assay, which further proved the interaction between circRPPH1 and FUS. (D) The co-immunoprecipitation assay verified the interaction of FUS and STAT3. (E) Western blot assay indicated that FUS knockdown poses no effect on the expression of STAT3. (F) Nuclear-cytoplasm separation assay indicated that circRPPH1 could promote the p-STAT3 levels in the nuclear, while FUS knockdown inhibited this effect. Data are presented as the mean ± SD. *P<0.05 and **P<0.01. circ-, circular; p-, phosphorylated.

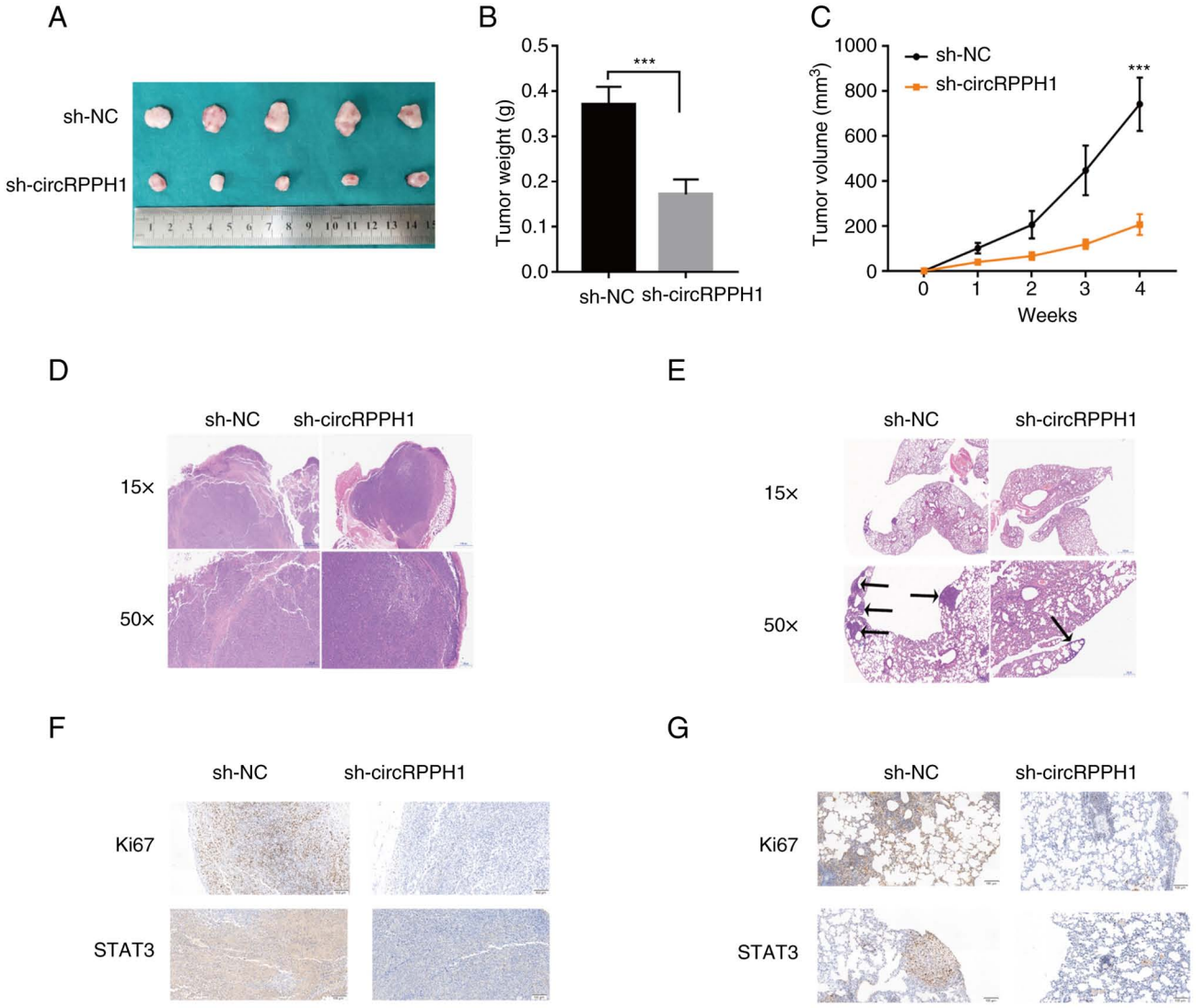

Figure 8. CircRPPH1 promotes growth and metastasis *in vivo*. (A-C) 5637 cells stably transfected with sh-circRPPH1 or vector were injected subcutaneously into the BALB/c nude mice. Tumor volume and weight were significantly decreased in sh-circRPPH1 group. (D) The subcutaneous tumors were identified by H&E staining. (E) Representative pictures of the lung metastasis. (F and G) The expression of Ki67 and STAT3 in tumors were analyzed by immunohistochemical assay (scale bar, 100 μm). Data are presented as the mean ± SD. ***P<0.001. circ-, circular; sh-, short hairpin; NC, negative control.

roles in the carcinogenesis of BCa and are potential treatment targets for BCa (29,30). With bioinformatics and cell biological analyses, it was revealed that circRPPH1, a 154-bp exonic circRNA, is highly expressed in BCa cells. However, its role and mechanism in BCa remain unclear.

Proliferation, migration and invasion are important characteristics of tumor cells and have important effects on tumor progression (31). The results of the present study suggested that the high expression of circRPPH1 in BCa could promote the proliferation, migration and invasion of cancer cells, while the downregulation of circRPPH1 could inhibit the proliferation, migration and invasion of BCa cells. It is worth noting that circRPPH1 has been reported to play an oncogenic role in breast cancer and glioblastoma, which indicates that the role of circRPPH1 in different types of tumors has certain commonalities (32-35).

miR-296-5p is considered to be an important tumor suppressor in colorectal cancer, non-small cell lung cancer, liver cancer and nasopharyngeal carcinoma, inhibiting cell proliferation, migration, invasion and epithelial-mesenchymal transition ((24,36-38). Particularly, circRPPH1 promotes cancer progression through the miR-296-5p/FOXP4 axis in breast cancer and through the miR-296-5p/RUNX1 axis in colorectal cancer, indicating that circRPPH1/miR-296-5p axis plays an important role in cancer malignancies (32,39). However, the role of circRPPH1/miR-296-5p axis in the malignant phenotype of BCa cells remains unclear. The present study confirmed that miR-296-5p could inhibit the proliferation, migration and invasion of BCa cells. Furthermore, circRPPH1 could exert oncogenic functions through miR-296-5p/STAT3 axis.

The JAK2/STAT3 signaling pathway, as a classical oncogenic signaling pathway, is widely involved in the migration, growth and differentiation of cancer cells (40). After JAK2 activation, downstream STAT3 can be activated to form p-STAT3 and promote the expression of downstream oncogenes. Numerous studies have reported that STAT3 can promote cell invasion by regulating EMT-related genes

and promote cell proliferation by inducing c-Myc transcription (41,42). In addition, the results of bioinformatics analysis in the present study showed that the expression of STAT3 was closely related to the pathological classification, pathological stage, histological grade and overall survival of BCa, which confirmed the cancer-promoting role of STAT3 in BCa.

Currently, there are certain studies suggesting that the interaction between RNA and protein may pose different effects on the nuclear translocation of related proteins, including the ability to aid or inhibit the nuclear translocation of proteins. For example, lncRNA OLA1P2 and circ-Amotl1 could inhibit or accelerate the nuclear translocation of the related binding proteins, respectively (9,43). FUS is a multi-function RNA-binding protein. In a recent study, the interaction between circSPARC and FUS was revealed to contribute to the nuclear translocation of p-STAT3 (26). In the present study, FUS is the only one RNA-binding protein (RBP) that binds with circRPPH1, and the interaction was confirmed by RIP assays. Furthermore, the interaction was also confirmed to promote the nuclear translocation of p-STAT3. Considering the complex and colorful functions of circRNAs, circRPPH1 may also exert its oncogene role in BCa by other pathways, which needs to be further confirmed.

There exist certain limitations to the present study. Firstly, only circRPPH1, a circRNA, was detected. However, there are a large number of differentially expressed circRNAs in BCa, and the role of these circRNAs in the occurrence and development of BCa requires further study. Secondly, whether circRPPH1 is involved in the occurrence and development of BCa through other mechanisms, such as regulating RNA selective splicing, still requires further investigation. It is expected that subsequent studies will further elucidate the role and mechanism of circRNA in BCa. In conclusion, circRPPH1 was firstly identified to play an oncogenic role in BCa progression. It was identified that circRPPH1 could upregulate STAT3 expression through sponging miR-296-5p, and interact with FUS to promote p-STAT3 nuclear translocation, thereby accelerating the proliferation, migration and invasion of BCa cells. CircRPPH1 could be a potential and promising treatment target for BCa.

Acknowledgements

Not applicable.

Funding

The present study was supported by the National Natural Science Foundation of China (grant nos. 81900645, 82170779 and 82270804), the Natural Science Foundation of Hubei Province (gran no. 2021CFB366), the 2019 Wuhan Yellow Crane Talent Program (Outstanding Young Talents) and the Tongji Hospital (HUST) Foundation for Excellent Young Scientist (grant no. 2020YQ15).

Availability of data and materials

The datasets used and/or analyzed during the current study are available from the corresponding author on reasonable request.

Authors' contributions

KT, ZC and XL designed the study. XL, YT and QH implemented the experiments. YH, HS and XL analyzed the data. TY and XL created the figures and tables. KT and XL drafted the article. KT and ZC confirm the authenticity of all the raw data. All authors revised the paper and read and approved the final version of the manuscript, and agreed to be accountable for all aspects of the work.

Ethics approval and consent to participate

This animal experiment was approved by the Animal Research Ethics Committee of Tongji Hospital (Wuhan, China).

Patient consent for publication

Not applicable.

Competing interests

The authors declare that they have no competing interests.

References

1. Siegel RL, Miller KD and Jemal A: Cancer statistics, 2020. CA Cancer J Clin 70: 7-30, 2020.
2. Luo C, Lei T, Zhao M, Meng Q and Zhang M: CD40 is positively correlated with the expression of nucleophosmin in cisplatin-resistant bladder cancer. J Oncol 2020: 3676751, 2020.
3. Knowles MA and Hurst CD: Molecular biology of bladder cancer: New insights into pathogenesis and clinical diversity. Nat Rev Cancer 15: 25-41, 2015.
4. Kristensen LS, Hansen TB, Venø MT and Kjems J: Circular RNAs in cancer: Opportunities and challenges in the field. Oncogene 37: 555-565, 2018.
5. Tong Y, Liu X, Xia D, Peng E, Yang X, Liu H, Ye T, Wang X, He Y, Xu H, *et al*: Biological roles and clinical significance of exosome-derived noncoding RNAs in bladder cancer. Front Oncol 11: 704703, 2021.
6. Zhang H, Xiao X, Wei W, Huang C, Wang M, Wang L, He Y, Sun J, Jiang Y, Jiang G and Zhang X: CircLIFR synergizes with MSH2 to attenuate chemoresistance via MutSα/ATM-p73 axis in bladder cancer. Mol Cancer 20: 70, 2021.
7. Xie F, Li Y, Wang M, Huang C, Tao D, Zheng F, Zhang H, Zeng F, Xiao X and Jiang G: Circular RNA BCRC-3 suppresses bladder cancer proliferation through miR-182-5p/p27 axis. Mol Cancer 17: 144, 2018.
8. Hansen TB, Jensen TI, Clausen BH, Bramsen JB, Finsen B, Damgaard CK and Kjems J: Natural RNA circles function as efficient microRNA sponges. Nature 495: 384-388, 2013.
9. Zeng Y, Du WW, Wu Y, Yang Z, Awan FM, Li X, Yang W, Zhang C, Yang Q, Yee A, *et al*: A circular RNA binds to and activates AKT phosphorylation and nuclear localization reducing apoptosis and enhancing cardiac repair. Theranostics 7: 3842-3855, 2017.
10. Ashwal-Fluss R, Meyer M, Pamudurti NR, Ivanov A, Bartok O, Hanan M, Evantal N, Memczak S, Rajewsky N and Kadener S: circRNA biogenesis competes with pre-mRNA splicing. Mol Cell 56: 55-66, 2014.
11. Legnini I, Di Timoteo G, Rossi F, Morlando M, Briganti F, Sthandier O, Fatica A, Santini T, Andronache A, Wade M, *et al*: Circ-ZNF609 is a circular RNA that can be translated and functions in myogenesis. Mol Cell 66: 22-37.e9, 2017.
12. Bromberg JF, Wrzeszczynska MH, Devgan G, Zhao Y, Pestell RG, Albanese C and Darnell JE Jr: Stat3 as an oncogene. Cell 98: 295-303, 1999.
13. Huynh J, Etemadi N, Hollande F, Ernst M and Buchert M: The JAK/STAT3 axis: A comprehensive drug target for solid malignancies. Semin Cancer Biol 45: 13-22, 2017.

14. Mirzaei S, Gholami MH, Mahabady MK, Nabavi N, Zabolian A, Banihashemi SM, Haddadi A, Entezari M, Hushmandi K, Makvandi P, *et al*: Pre-clinical investigation of STAT3 pathway in bladder cancer: Paving the way for clinical translation. Biomed Pharmacother 133: 111077, 2021.
15. Hindupur SV, Schmid SC, Koch JA, Youssef A, Baur EM, Wang D, Horn T, Slotta-Huspenina J, Gschwend JE, Holm PS and Nawroth R: STAT3/5 inhibitors suppress proliferation in bladder cancer and enhance oncolytic adenovirus therapy. Int J Mol Sci 21: 1106, 2020.
16. Zhong Z, Lv M and Chen J: Screening differential circular RNA expression profiles reveals the regulatory role of circTCF25-miR-103a-3p/miR-107-CDK6 pathway in bladder carcinoma. Sci Rep 6: 30919, 2016.
17. Li Y, Zheng F, Xiao X, Xie F, Tao D, Huang C, Liu D, Wang M, Wang L, Zeng F and Jiang G: CircHIPK3 sponges miR-558 to suppress heparanase expression in bladder cancer cells. EMBO Rep 18: 1646-1659, 2017.
18. Liu M, Wang Q, Shen J, Yang BB and Ding X: Circbank: A comprehensive database for circRNA with standard nomenclature. RNA Biol 16: 899-905, 2019.
19. Dudekula DB, Panda AC, Grammatikakis I, De S, Abdelmohsen K and Gorospe M: CircInteractome: A web tool for exploring circular RNAs and their interacting proteins and microRNAs. RNA Biol 13: 34-42, 2016.
20. McGeary SE, Lin KS, Shi CY, Pham TM, Bisaria N, Kelley GM and Bartel DP: The biochemical basis of microRNA targeting efficacy. Science 366: eaav1741, 2019.
21. Zeng J, Xiang W, Zhang Y, Huang C, Chen K and Chen Z: Ubiquitous expressed transcript promotes tumorigenesis by acting as a positive modulator of the polycomb repressive complex 2 in clear cell renal cell carcinoma. BMC Cancer 19: 874, 2019.
22. Livak KJ and Schmittgen TD: Analysis of relative gene expression data using real-time quantitative PCR and the 2(-Delta Delta C(T)) method. Methods 25: 402-408, 2001.
23. Yu CY and Kuo HC: The emerging roles and functions of circular RNAs and their generation. J Biomed Sci 26: 29, 2019.
24. Shi DM, Li LX, Bian XY, Shi XJ, Lu LL, Zhou HX, Pan TJ, Zhou J, Fan J and Wu WZ: miR-296-5p suppresses EMT of hepatocellular carcinoma via attenuating NRG1/ERBB2/ERBB3 signaling. J Exp Clin Cancer Res 37: 294, 2018.
25. Liang C, Zhao T, Li H, He F, Zhao X, Zhang Y, Chu X, Hua C, Qu Y, Duan Y, *et al*: Long non-coding RNA ITIH4-AS1 accelerates the proliferation and metastasis of colorectal cancer by activating JAK/STAT3 signaling. Mol Ther Nucleic Acids 18: 183-193, 2019.
26. Wang J, Zhang Y, Song H, Yin H, Jiang T, Xu Y, Liu L, Wang H, Gao H, Wang R and Song J: The circular RNA circSPARC enhances the migration and proliferation of colorectal cancer by regulating the JAK/STAT pathway. Mol Cancer 20: 81, 2021.
27. Berman HM, Westbrook J, Feng Z, Gilliland G, Bhat TN, Weissig H, Shindyalov IN and Bourne PE: The protein data bank. Nucleic Acids Res 28: 235-242, 2000.
28. Antoni S, Ferlay J, Soerjomataram I, Znaor A, Jemal A and Bray F: Bladder cancer incidence and mortality: A global overview and recent trends. Eur Urol 71: 96-108, 2017.
29. Sun K, Wang D, Yang BB and Ma J: The emerging functions of circular RNAs in bladder cancer. Cancers (Basel) 13: 4618, 2021.
30. Su Y, Feng W, Shi J, Chen L, Huang J and Lin T: circRIP2 accelerates bladder cancer progression via miR-1305/Tgf-β2/smad3 pathway. Mol Cancer 19: 23, 2020.
31. Hanahan D and Weinberg RA: Hallmarks of cancer: The next generation. Cell 144: 646-674, 2011.
32. Wang L, Wu H, Chu F, Zhang L and Xiao X: Knockdown of circ_0000512 inhibits cell proliferation and promotes apoptosis in colorectal cancer by regulating miR-296-5p/RUNX1 axis. Onco Targets Ther 13: 7357-7368, 2020.
33. Zhou Y, Liu X, Lan J, Wan Y and Zhu X: Circular RNA circRPPH1 promotes triple-negative breast cancer progression via the miR-556-5p/YAP1 axis. Am J Transl Res 12: 6220-6234, 2020.
34. Zhao C, Li L, Li Z, Xu J, Yang Q, Shi P, Zhang K and Jiang R: A novel circular RNA hsa_circRPPH1_015 exerts an oncogenic role in breast cancer by impairing miRNA-326-Mediated ELK1 inhibition. Front Oncol 10: 906, 2020.
35. Xiong JW, Song SB, Xiong LM, Duan CH, Song Q, Yu DL and Zhang XQ: CircRPPH1 promotes cell proliferation, migration and invasion of non-small cell lung cancer via the PI3K/AKT and JAK2/STAT3 signaling axes. J Biochem 171: 245-252, 2022.
36. Rong D, Lu C, Zhang B, Fu K, Zhao S, Tang W and Cao H: CircPSMC3 suppresses the proliferation and metastasis of gastric cancer by acting as a competitive endogenous RNA through sponging miR-296-5p. Mol Cancer 18: 25, 2019.
37. Savi F, Forno I, Faversani A, Luciani A, Caldiera S, Gatti S, Foa P, Ricca D, Bulfamante G, Vaira V and Bosari S: miR-296/Scribble axis is deregulated in human breast cancer and miR-296 restoration reduces tumour growth in vivo. Clin Sci (Lond) 127: 233-242, 2014.
38. Han W, Kong D, Lu Q, Zhang W and Fan Z: Aloperine inhibits proliferation and promotes apoptosis in colorectal cancer cells by regulating the circNSUN2/miR-296-5p/STAT3 pathway. Drug Des Devel Ther 15: 857-870, 2021.
39. Yang L, Liu Z, Ma J, Wang H, Gao D, Zhang C and Ma Q: CircRPPH1 serves as a sponge for miR-296-5p to enhance progression of breast cancer by regulating FOXP4 expression. Am J Transl Res 13: 7556-7573, 2021.
40. Yu H, Lee H, Herrmann A, Buettner R and Jove R: Revisiting STAT3 signalling in cancer: New and unexpected biological functions. Nat Rev Cancer 14: 736-746, 2014.
41. Shen M, Xu Z, Xu W, Jiang K, Zhang F, Ding Q, Xu Z and Chen Y: Inhibition of ATM reverses EMT and decreases metastatic potential of cisplatin-resistant lung cancer cells through JAK/STAT3/PD-L1 pathway. J Exp Clin Cancer Res 38: 149, 2019.
42. Jin W: Role of JAK/STAT3 signaling in the regulation of metastasis, the transition of cancer stem cells, and chemoresistance of cancer by epithelial-mesenchymal transition. Cells 9: 217, 2020.
43. Guo H, Liu J, Ben Q, Qu Y, Li M, Wang Y, Chen W and Zhang J: The aspirin-induced long non-coding RNA OLA1P2 blocks phosphorylated STAT3 homodimer formation. Genome Biol 17: 24, 2016.